ISSN 1063-7710, Acoustical Physics, 2010, Vol. 56, No. 6, pp. 935–941. © Pleiades Publishing, Ltd., 2010.

Control of the Self-Assembly Processes in a Droplet of a Colloidal Solution by an Acoustic Field

O. V. Rudenko[a], P. V. Lebedev-Stepanov[b], V. A. Gusev[a], A. I. Korobov[a], B. A. Korshak[a], N. I. Odina[a], M. Yu. Izosimova[a], S. P. Molchanov[b], and M. V. Alfimov[b]

[a] *Faculty of Physics, Moscow State University, Moscow, 119991 Russia*

e-mail: vgusev@bk.ru

[b] *Center of Photochemistry, Russian Academy of Sciences, ul. Novatorov 7a, Moscow, 119421 Russia*

Received May 11, 2010

Abstract—The formation of structured films consisting of ensembles of micro- or nanoparticles and possessing preset functional characteristics is studied both experimentally and theoretically. The films are obtained by drying out droplets of colloidal solutions on a solid substrate under the acoustic effect produced by a standing SAW field.

DOI: 10.1134/S1063771010060187

INTRODUCTION

Ordered ensembles of micro- and nanoparticles obtained by the method of self-assembly from colloidal solutions form structures of the type of photonic crystals. They are used in optical devices, chemosensor elements, flexible protecting layers for light-emitting diodes, etc.

The self-assembly in the course of solvent evaporation occurs owing to capillary forces, which displace the particles in the near-surface layers of the solution as the volume of the latter decreases. By presetting the external parameters of the process (pressure, temperature, and humidity) and its internal parameters (concentration of the solution, materials of the substrate and the particles, type of the solvent, and size and shape of the particles), it is possible to affect the result of the self-assembly, namely, the morphology of the solid phase.

A droplet drying on a substrate represents an open dissipative system in which self-organization processes occur in the course of the solvent evaporation [1] and the dissolved substance may crystallize or settle by forming ordered solid structures [2]. The dynamics of droplets drying within time intervals from tens of hours to fractions of seconds (depending on the droplet size, from a centimeter to several tens of microns) has been investigated in [2–9].

From the point of view of technological applications, it is important to control the nanoparticle ordering process. For this purpose, it is possible, for example, to use structured substrates with a surface relief, which can be made by plasma etching or laser lithography. In the latter case, the characteristic scale of the relief is determined by the optical wavelength and is usually on the order of 1 μm. Another method consists in depositing the initial layer of nanoparticles on the substrate. In this case, the relief of the initial layer depends on the type of packing and the size and shape of particles. The second layer is deposited on the initial layer. The particle arrangement in the second layer is determined by the relief of the initial layer and by its adhesion to the substrate; however, the second layer may cause some molecule displacements in the initial layer.

These methods of control do not involve application of external fields and can be called "passive" methods. An example of an "active" method is the use of a rotating substrate (spin coating or centrifugation). This method uses the inertial forces to make the particles form a film that is smoother and more homogeneous in thickness.

The application of an acoustic field is the next step in the development of self-assembly control methods. Although the acoustic field has been much used for structuring various solutions [10, 11], its use for controlling the self-assembly processes in a droplet of a colloidal solution represents a new approach [12, 13].

The application of the acoustic field is expedient for the following reasons [14].

(i) Self-assembly can be intensified by the vibration effect on both the particles and the substrate. When the drying solution is shaken, the mobility of nanoparticles increases and the formation of a denser packing is more probable.

(ii) A field with a complex configuration can be obtained, e.g., by exciting a standing acoustic wave. In this case, the ensemble of particles is separated into groups with reduced and increased numbers of particles, which allows the formation of ordered structures.

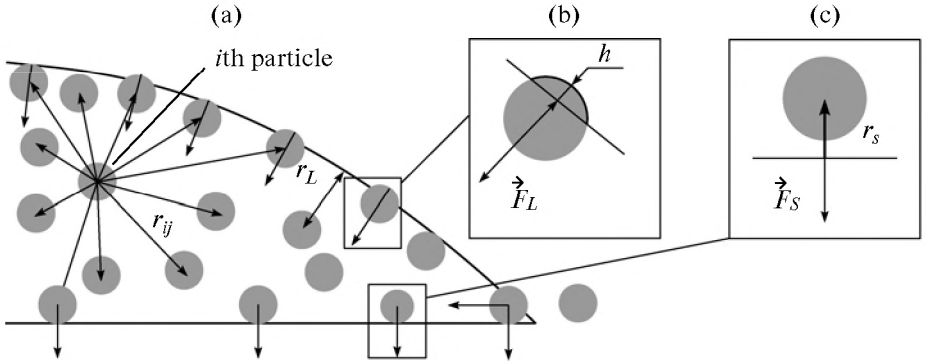

Fig. 1. Particle interaction forces in a droplet: (a) the liquid–air interaction (a spherical segment) and the displacement of particles in the course of evaporation, (b) the interaction force between the particles and the surface layer of the droplet, and (c) the interaction of the particles with the substrate [3].

(iii) A directional transport can be created; i.e., the particles can be transferred from one part of the specimen to another.

(iv) The wavelength and the intensity of acoustic waves can be varied over wide limits so as to optimize the acoustic effect and to create structures with preset properties.

In this paper, we investigate the possibilities of the formation of ordered structures from nanoparticles as a result of the self-assembly process that occurs under the effect of acoustic vibrations. Special attention is paid to determining the factors that affect the parameters and the quality of the resulting specimens, as well as to the choice of the optimal configuration of the experimental setup.

In our study, the acoustic effect on a droplet is produced by a standing surface acoustic wave (SAW) excited in the solid substrate.

THEORY

For theoretical description of the system under study, it is necessary to analyze the following processes.

(i) Evaporation of a droplet or a film of a colloidal solution on a flat substrate. The droplet of a given size has the shape of a spherical segment the parameters of which are determined by the wetting angle of the solution on the substrate. The evaporation of the solvent is caused by diffusion of the solvent vapor from the droplet surface to the atmosphere.

(ii) The motion of nanoparticles inside an evaporating sessile droplet of a colloidal solution under the effect of the acoustic field.

To describe the motion of colloidal particles in a viscous medium (liquid), the approach based on dissipative particle dynamics has been developed [3, 15]. This approach is analogous to that of molecular dynamics, but, instead of molecules, it considers nanoparticles moving in a continuous medium, i.e., the solvent, which is characterized by the mean density, viscosity, and permittivity. In a colloidal solution, a particle experiences the effect of the following forces [3]: the resultant conservative force acting from the side of other particles, the interaction force between the particle and the substrate, the capillary force responsible for the interaction of the particle with the solution–air interface, and the force that is caused by the interaction with the solvent and depends on the viscosity and the density ratio between the particle and the solution (Fig. 1). In the presence of an external field (the acoustic field in the case under study), the corresponding force should be included in the equation.

Thus, the motion of any ith particle is described by the Langevin equation

$$m\frac{d\mathbf{v}_i}{dt} = \sum_j \mathbf{F}_{ij} + \mathbf{F}_D + \mathbf{F}_B + \mathbf{F}, \quad (1)$$

where, on the left-hand side, we have the product of the mass of the ith particle $m = (4/3)\pi R^3\rho_p$ by its acceleration; on the right-hand side, one can see the sum of conservative forces acting on the particle $\sum_j \mathbf{F}_{ij}$, the dissipative force $\mathbf{F}_D$, the random Brownian force $\mathbf{F}_B$, and the external force $\mathbf{F}$.

The first term on the right-hand side of Eq. (1) describes the interaction of particles with one another and with the interfaces (Fig. 1). The second term is of hydrodynamic and kinetic origin: it describes the interaction of a particle with the solvent, namely, the viscous friction and the particle entrainment by the solvent flow. The Brownian force $\mathbf{F}_B$ is caused by thermal motion and has a Gaussian distribution with zero mean and with the mean square deviation determined by the formula

$$\langle F_{B,i}^2 \rangle = 2\pi\eta akT/\tau.$$

Here, k is the Boltzmann constant, T is the temperature, a is the particle radius, τ is the step in time, and η is the viscosity of the solution. The last term on the right-hand side of Eq. (1) is responsible for the external forces applied to the particle. In our case, this is the force generated by the acoustic field.

The colloidal particles in an aqueous solution used for self-assembly often acquire a surface electric charge (positive or negative, depending on the properties of molecules on the particle surface) and an ion sheath compensating this charge. The interaction of such particles in the far zone is described by the partially screened Coulomb repulsive potential, whereas, in the near zone, Van der Waals intermolecular forces predominate.

Because of the Coulomb repulsion, the particles tend to separate from each other in the solution; however, if they collide, they may form complexes.

The approach that corresponds to the classical Deryagin–Landau–Verwey–Overbeek theory [16–19] describes the electrostatic interaction by the Debye–Hückel potential

$$U_{DH}(r) = \frac{C}{r}\exp(-\lambda r), \quad \lambda^2 = \frac{1}{\varepsilon\varepsilon_0 kT}e^2\sum_i z_i^2 n_{i0}.$$

Here, C is determined as

$$C = \frac{z^2e^2}{4\pi\varepsilon\varepsilon_0}\left[\frac{\exp(\lambda R)}{1+\lambda R}\right]^2,$$

where λ is the inverse Debye screening length, which depends on the ionic strength of the solution; ze is the average electric charge corresponding to a particle; ε is the relative permittivity of the solution; ε_0 is the dielectric constant (in the SI system of units); and n_{i0} is the concentration of ions of the ith type in the solution.

For the dispersive attraction force potential integrated over the atoms of the interatomic potential, the following expression was proposed [19]:

$$U_{\mathrm{VDW}} = U_{\mathrm{HS}} - \frac{A}{12}\left[\frac{a^2}{r^2-a^2} + \frac{4r^2}{(2a)^2} + 2\ln\left(1-\frac{a^2}{r^2}\right)\right],$$

where r is the distance between the particle centers, a is the particle radius, A is the Hamaker constant, and U_{HS} is the potential of a rigid sphere.

Let us consider in more detail the external force due to the acoustic action (Fig. 2).

Piezoelectric elements (interdigital transducers) generate surface waves propagating in opposite directions and forming a standing wave. As a result, in the droplet, rapidly oscillating (usually, at frequencies of 10–100 MHz) pressure and oscillation velocity fields are formed with fixed positions of nodes and antinodes. The average acoustic pressure within the oscillation period is zero, and, therefore, slow motions and grouping of particles occur under the effect of radiative

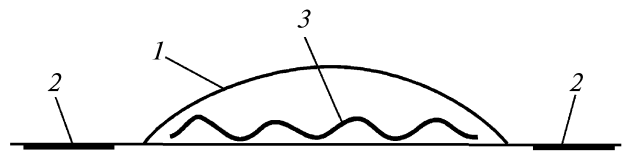

Fig. 2. Droplet of the solution in the acoustic field: (*1*) the droplet surface, (*2*) the piezoelectric elements generating the acoustic field, and (*3*) the standing acoustic wave.

forces [20], which are quadratic in the acoustic variables:

$$F_i = \frac{\partial}{\partial x_k}\left(\frac{\varepsilon}{c^2\rho}\langle p'^2\rangle\delta_{ik} + \rho\langle u_i u_k\rangle\right). \tag{2}$$

Here, p' and u_i are the acoustic pressure and velocity fields and c, ρ, and ε are the velocity of sound, the density, and the nonlinearity parameter of the medium. The angular brackets denote averaging over the fast time, i.e., the period of the acoustic wave. To calculate the radiation pressure under the experimental conditions, it is sufficient to calculate the acoustic fields in the linear approximation.

For simplicity, we replace the actual droplet on a solid substrate by a plane liquid layer. The substrate occupies the half-space $z > 0$, and the layer occupies the region $-h < z < 0$. The x axis is directed along the interface. The idea of calculating the acoustic fields in such a system was described in [22, 23]. It is as follows. When a surface wave propagates along the interface, acoustic fields are formed in both media. In the liquid layer, the field is represented by two longitudinal waves the wave vectors of which have opposite directions of their projections on the normal: upward and downward. In the solid substrate, the field is formed by the combination of longitudinal and transverse waves of a special type. These four components of the acoustic field are determined from the corresponding wave equations, the solutions of which are related by four boundary conditions.

Three conditions are set at the boundary between the substrate and the liquid layer at $z = 0$. They include the equality of vertical displacements in the two media; the equality of normal stresses (the stress tensor component is identical to pressure with the minus sign: $\sigma_{zz} = -p'$), and the zero value of tangential stresses in the solid (the liquid is assumed to be ideal). The fourth condition is set at the upper (free) boundary of the liquid layer: at $z = -h$, the acoustic pressure is $p' = 0$.

Substituting the solution for traveling waves in these conditions, we obtain the dispersion equation for the velocity of the surface wave:

$$k^2qs - (k^2+s^2)^2 = \frac{\rho_0}{\rho}qk_t^4\begin{cases} r^{-1}\tan(rh) \\ r_*^{-1}\tanh((r_*h). \end{cases}$$

The upper row on the right-hand side corresponds to such a solution to the dispersion equation that the wave velocity in the system c is greater than the velocity of sound in the liquid c_0 and smaller than the velocities of the longitudinal c_l and transverse c_t waves in the solid: $c > c_0$, $c < c_t < c_l$. The lower row on the right-hand side corresponds to the wave velocity smaller than the velocity of sound in the liquid: $c < c_0$. In addition, $r = ir_*$, $r_* = \sqrt{k^2 - k_0^2}$. Here, we used the following notations: $k = \omega/c$ is the horizontal component of the wave number of the surface wave; $k_0 = \omega/c_0$, $k_l = \omega/c_l$, and $k_t = \omega/c_t$ are the wave numbers of traveling waves in the liquid and in the solid; $q^2 = k^2 - k_l^2$, $s^2 = k^2 - k_t^2$, and $r^2 = k_0^2 - k^2$; h is the thickness of the liquid layer; and ρ_0 and ρ are the densities of the liquid and the substrate, respectively.

The expression for the acoustic field potential in the liquid layer has the form

$$\varphi = -i\omega\frac{q}{r}\frac{k_t^2}{k^2+s^2}\frac{\sin r(z+h)}{\cos rh}e^{-i(\omega t - kx)}A, \qquad (3)$$

where A is an arbitrary amplitude. Knowing potential (3), we can easily determine the oscillation velocity $\mathbf{u} = \nabla\varphi$ and the acoustic pressure $p' = i\omega\rho_0\varphi$.

If two opposite waves of type (3) are excited in the system, a standing surface wave is formed with the potential

$$\varphi = -i\omega A\frac{2q}{r}\frac{k_t^2}{k^2+s^2}\frac{\sin r(z+h)}{\cos rh}\cos kx e^{-i\omega t}.$$

Now, we can calculate the oscillation velocity and acoustic pressure fields; then, using Eq. (2), we determine the radiation force. The force proves to be a potential one. It can be represented in the form $\mathbf{F} = -\nabla U$, where

$$\frac{U}{U_0} = (\varepsilon - 1)\frac{k_0^2}{r^2}[\cos 2r(z+h) - 1]\cos 2kx - \cos 2kx$$

$$+\left[(\varepsilon - 1)\frac{k_0^2}{r^2} + \frac{k^2}{r^2}\right]\cos 2r(z+h), \qquad (4)$$

$$U_0 = \frac{\rho_0}{8}\left(\frac{2\omega q}{\cos rh}\frac{k_t^2}{k^2+s^2}\right)^2 A^2.$$

Potential (4) depends on both horizontal and vertical coordinates. At a fixed horizontal coordinate, the potential reaches its minimum at the lower boundary of the layer. The potential relief given by Eq. (4) is periodic along the substrate with the period $x_* = \pi/k = c/2f$, which makes half of the acoustic wavelength.

Thus, we calculated the potential (Eq. (4)) of radiation forces acting on a liquid volume element. However, we are interested in the force acting on the particles suspended in the liquid. If the size of these particles is sufficiently large, they will experience radiation pressure of other origin related to the anisotropic scattering of the acoustic field [24, 25]. It is known that the intensity ratio between the scattered field and the incident wave is on the order of $(R/\lambda)^4$ [20], where R is the particle radius. In the case of small particles, the scattering is weak and the particles themselves are almost completely entrained by the liquid. For example, under the conditions of one of our experiments, where polystyrene particles with a radius of about 100 nm were used and the wavelength at a frequency of 15 MHz was 240 μm, the scattered field was on the order of 10^{-13}. Hence, the predominant mechanism acting on the suspended particles was their entrainment by the liquid, which was set in motion by radiative force (4).

It can be shown [13] that, if the densities of a particle and the medium are close to each other, their velocities are approximately identical and the particle displacement with respect to the liquid is approximately zero. Since the time average displacement of the liquid under the acoustic action is zero, the particles suspended in the liquid will not be shifted in space. However, the motion in the field of radiation forces (4) is more complicated. The sound field generates hydrodynamic flows in the droplet, and these flows entrain the suspended particles. The particles are grouped under the effect of the acoustically induced convection, which to a considerable extent determines the morphology of the ordered structures formed on the substrate after the liquid dries out. In large droplets and thick films, the development of instabilities violating the contrast of the resulting structure is possible. Additional streaming due to shape oscillations of the droplet may also arise [26].

COMPUTER SIMULATION

On the basis of the physical model described above, a computer program was developed for numerical simulation of the self-assembly of nanoparticles in the acoustic field. We calculated the multidimensional trajectory of the system (the ensemble of particles) $\mathbf{r}_i = \mathbf{r}_i(t)$, $i = 1, 2, ..., N$. We analyzed both the self-assembly process and its result: from the initial state to the terminal state at $t = t_{\max}$.

The time of calculating the evolution of the system from initial to terminal state strongly depends on the number of particles in the system. The acceptable time of calculation by an ordinary PC allows tracing the motion of several hundreds of particles. In this case, it is possible to reconstruct the main features of the acoustic effect on microdroplets containing relatively small numbers of particles.

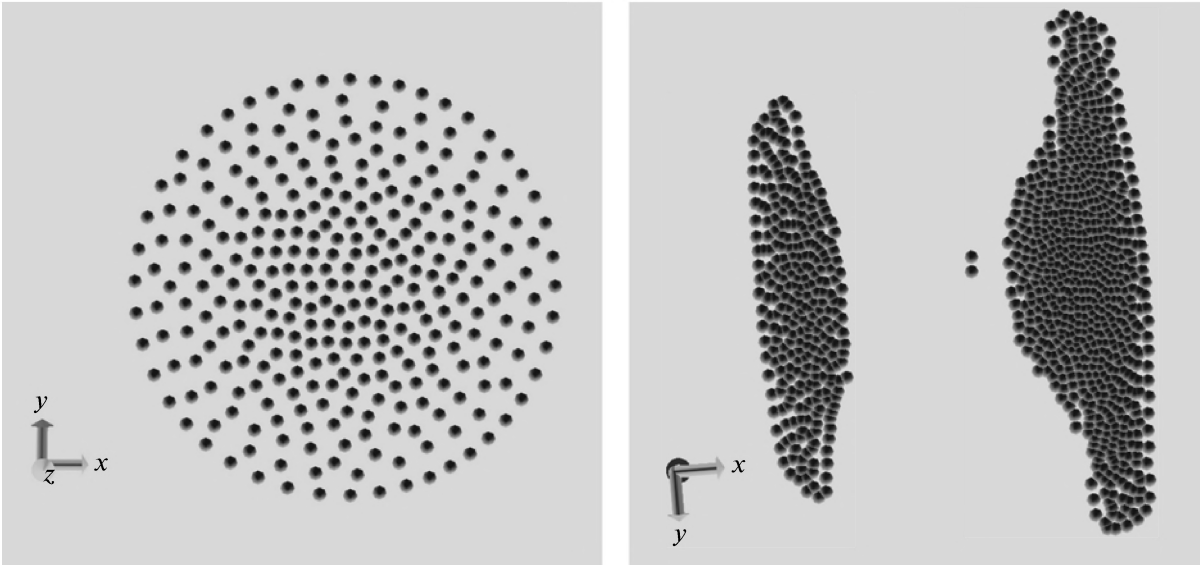

Fig. 3. Visualization of the distribution of 300 particles on the substrate according to the data of the numerical experiment: without the acoustic field (left) and in the presence of the acoustic field (right).

Figure 3 shows the results of calculations for an ensemble of 300 silicon dioxide particles with a diameter of 1 μm each; the patterns are formed as a result of drying of a droplet with an initial volume of 40 pl in the absence of the external field (left) and under the controlling acoustic action (right). Visualization was performed using the VMD1.8 program open to users. The diameter of the ensemble is 100 μm. One can see that, in the absence of acoustic action, a characteristic circular structure is formed with the density of particles increasing steadily toward the center. No ordering with formation of a preferential direction is observed. Under the effect of the external acoustic field, the structure is radically different. A nonuniform distribution of particle concentration appears in the direction of acoustic field variation: one can see regions where particles are scarce and regions where most of the particles are concentrated. The particles are concentrated around the minima of the radiation pressure potential. The asymmetry of the structure is related to the asymmetric orientation of the acoustic field with respect to the droplet.

THE EXPERIMENTAL TECHNIQUE AND SETUP

The experimental setup used for studying the formation of nanoparticle ensembles is schematically represented in Fig. 4. The sound channel (the SAW line) was an optically polished YZ-cut lithium niobate crystal with interdigital transducers (IDT1 and IDT2) on its surface. To provide the measurements in a wide frequency range, several sound channels were used. The SAW frequency was within 15–150 MHz, and the loss due to the double conversion did not exceed 20 dB. The SAW wavelength at a frequency of 15 MHz was 240 μm. The studies were carried out in a continuous mode of operation. A source of radio signals generated a continuous signal in the form of alternating high-frequency voltage, which, after amplification to 1–10 V, was supplied to IDT1 and IDT2. The frequency and amplitude of the voltage was monitored by an oscilloscope. As a result of the propagation of two surface acoustic waves in opposite directions, an acoustic field in the form of a standing SAW was generated. In the standing wave field, a droplet of a solution containing suspended nanoparticles was placed. The initial size of the droplet was about 5 mm. In the experiments, we used aqueous solvents. As nanoparticle materials, we used polystyrene and silicon dioxide (SiO_2). The polystyrene particles had a density of about 1.05 g/cm^3, and the silicon dioxide particles, about 2 g/cm^3. We also studied a Ca_2CO_3 powder containing particles of different size: (1–3) μm. In the standing wave field, the nanoparticles were grouped in the regions corresponding to the minima of the radia-

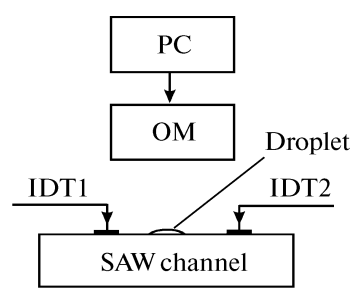

Fig. 4. Schematic representation of the experimental setup.

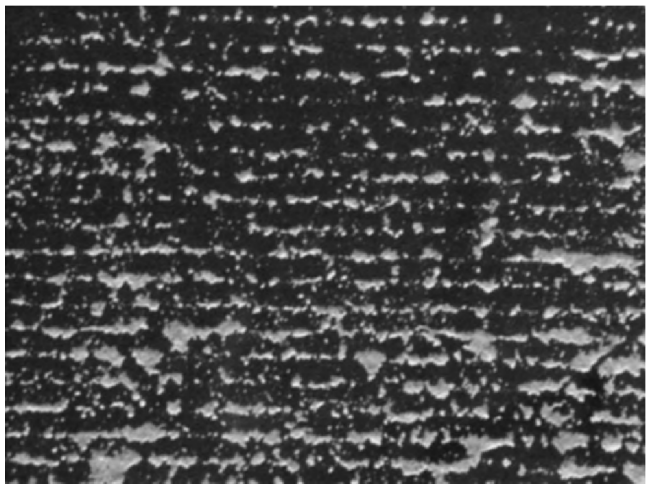

Fig. 5. Ca_2CO_3 powder. The droplet diameter is 7 mm, the solvent is water, and the mass concentration of the solution is 4%. The SAW frequency is 15 MHz, and the SAW wavelength is 240 μm. The distance between the maxima of the structure is 120 μm.

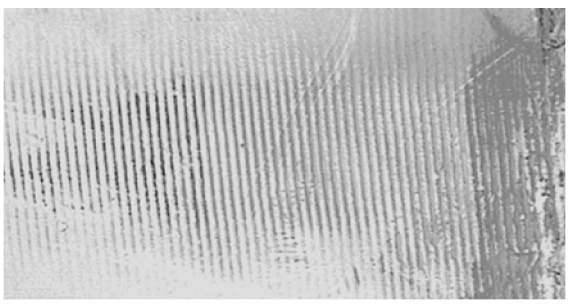

Fig. 6. SiO_2 particles with a diameter of 6 μm. The droplet diameter is 2.5–3 mm, the solvent is water, and the initial mass concentration of the solution is 4%. The SAW frequency is 45 MHz, and the SAW wavelength is 80 μm. The distance between the maxima is 40 μm.

tion pressure potential. After the evaporation of the liquid, on the surface of the sound channel we observed ordered ensembles of nanoparticles with a period identical to half of the SAW wavelength. An optical microscope (OM) mounted above the sound channel and connected with the PC allowed us to visually observe the formation of structures and measure and record their geometric parameters.

EXPERIMENTAL RESULTS

Figure 5 shows a photograph of an ensemble of Ca_2CO_3 particles deposited from the aqueous solution in the standing SAW field with a frequency of 15 MHz and a wavelength of 240 μm. The size of the particles varied within 1–3 μm. From Fig. 5, one can see that, after evaporation of the liquid, a periodic structure with a period of 120 μm is formed from particles on the surface of the sound channel. Figure 6 shows the photograph of an ensemble of silicon dioxide (SiO_2) particles formed after drying of an alcoholic solution in the standing SAW field with a frequency of 45 MHz and a wavelength of 80 μm. The particle size was 200 nm. One can clearly see the structure with a period of 40 μm.

First of all, we note the coincidence of the experimental data with the main theoretical result: the spatial period of the structure formed from nanoparticles is identical to half the acoustic wavelength. Thus, the assumption that, in the presence of the acoustic action, the main ordering factor is the radiation pressure in the liquid proves to be experimentally verified.

The structure consisting of Ca_2CO_3 particles that is shown in Fig. 5 allows us to conclude that the formation of an ordered structure is possible even for an ensemble of particles widely scattered in size, the period of the structure being still identical to half the wavelength. However, the pattern is somewhat vague and the lines are not smooth, which can be explained by both the considerable scatter in size and the specific features of interactions between the Ca_2CO_3 particles.

The use of particles of the same size (silicon dioxide, Fig. 6) allowed us to obtain a clearly defined structure. In addition, we observed a tendency toward formation of a more clear-cut structure with decrease in the particle size and with the increase in the frequency of the acoustic action. The results allow us to conclude that a decrease in the particle size and an increase in the SAW frequency lead to the formation of structures with well-defined boundaries.

The maximal effect of the acoustic field was observed for the particles the density of which was noticeably different from the density of the solvent (water).

The Ca_2CO_3 powder showed sufficiently evident results (Fig. 5). It was well sorbed on the substrate, where the radiative forces are maximal. On the other hand, for polystyrene particles with a density of 1.05 g/cm^3, the effect of the acoustic field was less pronounced. The density of the silicon dioxide particles was almost twice as great as the density of water, although the presence of pores in these particles slightly reduced their effective density. In this case, a perfectly clear structure was formed (Fig. 6).

CONCLUSIONS

We experimentally demonstrated the possibility of an acoustic control of the self-assembly process in an ensemble of colloidal particles. The control was implemented by varying the configuration and intensity of the acoustic wave and also by varying the properties of the particles and the solvent. The experimental data agree well with the conclusions of the physical model developed for describing the process and with the results of computer simulations. The model explains the basic properties of the resulting struc-

tures, such as the spatial period and the dependence of the acoustic effect produced on the particles on the density ratio between the particles and the solvent.

ACKNOWLEDGMENTS

We are grateful to Yu.N. Makov and N.A. Chernyshov for cooperation in the project. This work was supported by the Federal Agency of Science and Innovations (state contract no. 02.513.12.3028) and the Russian Foundation for Basic Research (project no. 09-03-12117).

REFERENCES

1. G. Nikolis and I. Prigogine, *Self-Organization in Non-Equilibrium Systems* (Wiley, New York, 1977; Mir, Moscow, 1979).
2. L. V. Andreeva, D. A. Ivanov, D. S. Ionov, D. S. Ionov, A. V. Koshkin, P. V. Lebedev-Stepanov, O. Yu. Rybakov, A. S. Sinitskii, A. N. Petrov, and M. V. Alfimov, Prib. Tekh. Éksp., No. 6 (2006) [Instrum. Exp. Tech. **49**, 860 (2006)].
3. L. V. Andreeva, A. V. Koshkin, P. V. Lebedev-Stepanov, A. N. Petrov, and M. V. Alfimov, Colloids Surf. A: Physicochem. Eng. Aspects **300**, 300 (2007).
4. Yu. Yu. Tarasevich, Usp. Fiz. Nauk **174**, 779 (2004) [Phys. Usp. **47**, 717 (2004)].
5. H. Hu and R. G. Larson, Langmuir **21**, 3972 (2005).
6. H. Hu and R. G. Larson, Langmuir **21**, 3972 (2005).
7. R. Deegan, Phys. Rev. E **61**, 475 (2000).
8. R. Deegan, O. Bakajin, T. Dupont, G. Huber, S. Nagel, and T. Witten, Phys. Rev. E **62**, 756 (2000).
9. M. V. Alfimov, R. M. Kadushnikov, N. A. Shturkin, V. M. Alievskii, and P. V. Lebedev-Stepanov, Ross. Nanotekhnol. **1**, 127 (2006).
10. A. Alvarez, J. Friend, and L. Y. Yeo, Nanotechnology **19**, 455103 (2008).
11. A. Alvarez, J. Friend, and L. Y. Yeo, Langmuir **24**, 10629 (2008).
12. P. V. Lebedev-Stepanov and S. A. Rybak, Akust. Zh. **55**, 326 (2009) [Acoust. Phys. **55**, 329 (2009)].
13. P. V. Lebedev-Stepanov and O. V. Rudenko, Akust. Zh. **55**, 706 (2009) [Acoust. Phys. **55**, 729 (2009)].
14. O. V. Rudenko, P. V. Lebedev-Stepanov, A. I. Korobov, B. A. Korshak, S. P. Molchanov, and M. V. Alfimov, Ross. Nanotekhnol., Nos. 7–8 (2010).
15. P. J. Hoogerbrugge et al., Europhys. Lett. **19**, 155 (1992).
16. B. V. Derjaguin and L. Landau, Acta Physicochim. USSR **14**, 633 (1941).
17. E. J. W. Verwey and J. Th. Overbeek, *Theory of the Stability of Lyophobic Colloids* (Elsevier, Amsterdam, 1948).
18. L. B. Boĭnovich, Usp. Khim. **76**, 510 (2007).
19. V. I. Roldugin, Usp. Khim. **73**, 123 (2004).
20. O. V. Rudenko and S. I. Soluyan, *Theoretical Foundations of Nonlinear Acoustics* (Nauka, Moscow, 1975; Consultants Bureau, New York, 1977).
21. Z. A. Gol'dberg, in *Strong Ultrasonic Fields*, Ed. by L. D. Rozenberg (Nauka, Moscow, 1968) [in Russian].
22. I. A. Viktorov, *Sonic Surface Waves in Solids* (Nauka, Moscow, 1981) [in Russian].
23. V. A. Gusev and O. V. Rudenko, Akust. Zh. **56** (6) (2010, in press).
24. L. P. Gor'kov, Dokl. Akad. Nauk SSSR **140**, 88 (1961) [Sov. Phys. Dokl. **6**, 773 (1961)].
25. *Acoustics in Problems*, Ed. by S. N. Gurbatov and O. V. Rudenko (Fizmatlit, Moscow, 2009) [in Russian].
26. M. A. Ilyukhina and Yu. N. Makov, Acoust. Phys. **55**, 722 (2009).

Translated by E. Golyamina